Testing the validity of a mechanism describing the oxidation of binary *n*-heptane/toluene mixtures at engine operating conditions

Zisis Malliotakis [a],*, Colin Banyon [b], Kuiwen Zhang [c], Scott Wagnon [c], Jose Juan Rodriguez Henriquez [d], George Vourliotakis [a], Christos Keramiotis [a], Maria Founti [a], Fabian Mauss [d], William J. Pitz [c], Henry Curran [b]

[a] *Laboratory of Heterogeneous Mixtures and Combustion Systems, School of Mechanical Engineering, National Technical University of Athens, Heroon Polytechniou 9,15780, Athens, Greece*
[b] *Combustion Chemistry Centre, School of Chemistry, Ryan Institute, National University of Ireland, Galway, Ireland*
[c] *Lawrence Livermore National Laboratory, Livermore, CA 94551, USA*
[d] *Thermodynamics and Thermal Process Engineering, Brandenburg University of Technology, Cottbus, Germany*

ARTICLE INFO

ABSTRACT

The aim of this work is to evaluate the influence of the *n*-heptane/toluene ratio on the reactivity of binary toluene reference fuels (TRFs), through a combined experimental and numerical work. Novel experimental ignition delay time (IDT) data of three binary TRFs of varying *n*-heptane/toluene ratios have been obtained in a high-pressure shock tube and in a rapid compression machine at conditions relevant to novel engine operation. Measurements have been performed at two pressures (10 and 30 bar), and at three fuel/air equivalence ratios (0.5, 1.0 and 2.0) for TRF mixtures of 50%, 75% and 90% by volume toluene concentration, over the temperature range of 650–1450 K. It was found that, increasing the *n*-heptane content, led to an increase in reactivity and shorter measured IDTs. Reduced sensitivity to the equivalence ratio was observed at high temperatures, especially for high toluene content mixtures. A well validated detailed kinetic mechanism for TRF oxidation was utilized to provide further insight into the experimental evidence. The mechanism, which has recently been updated, was also assessed in terms of its validity, contributing thus to its continuous development. Reaction path analysis was performed to delineate critical aspects of toluene oxidation under the considered conditions. Further, sensitivity analysis highlighted the interactions between the chemistry of the two TRF components, revealing toluene's character as a reactivity inhibitor mainly through the consumption of $\dot{O}H$ radicals.

1. Introduction

Efficient and clean combustion of hydrocarbons has always attracted the attention of the scientific community. Spark ignition (SI) and compression ignition (CI) engines are the two most common types of internal combustion engines (ICEs) which make use of real (i.e. being the outcome of a distillation process in a refinery) gasoline and diesel fuels, respectively. These fuels are complex mixtures of several hydrocarbon families [1] and hence, simplified mixtures, denoted as fuel surrogates, are used to emulate their properties. The most common fuel surrogates for the combustion of real gasoline and diesel fuels consist mainly of the so-called primary reference fuels (PRFs), i.e. mixtures of *iso*-octane

and *n*-heptane, which have research octane numbers (RONs) of 100 and 0, respectively. Matching the octane numbers, both research (RON) and motored (MON) [2], of the actual fuel is a measure of a fuel's resistance to auto-ignite under a compression ignition engine environment [3]. As engine technology has moved towards unconventional low-temperature combustion (LTC) operating modes, PRF blends have proven to be inadequate in describing a real fuel's behavior e.g. [4]. This has also been attributed to the fact that PRF blends exhibit zero sensitivity i.e. RON = MON [5]. A fuel's sensitivity, defined as the difference between the RON and MON values, was found to be more important than the sole values of RON and MON as it described the auto-ignition performance throughout a wide temperature regime, not only at the temperatures of interest for conventional gasoline and diesel engines e.g. [6,7]. In an attempt to capture the behavior of real transportation fuels in engines operating under LTC modes, PRF fuels were

blended with toluene, the simplest methylated aromatic species, creating so-called toluene reference fuels (TRFs) [8,9]. TRF is a generic term frequently used to define binary or ternary mixtures of toluene with either or both *n*-heptane and *iso*-octane, and in the present study it is used to denote binary toluene and *n*-heptane mixtures. It should also be noted that toluene has often been used as a measure of anti-knock since it exhibits very high RON and MON numbers, between 116–120 and 103–110, respectively [8,10–12].

Toluene oxidation has attracted a lot of attention as a single component which has yielded a large number of studies, both experimental and numerical. A detailed list of toluene related work has been reported previously by Metcalfe et al. [13]. Speciation data at atmospheric pressure for fuel-lean and fuel-rich mixtures were measured in both a flow- reactor [14] and in a jet-stirred reactor [15]. These two studies have served as validation targets and were subsequently used for model development purposes. The former dataset was utilized for the development of a sub-model for benzene and toluene oxidation with 68 and 62 additional reactions [16], while the second study included a model containing 120 species and 920 reactions [15]. Flow reactor species measurements and model development were also carried out by Bounaceur et al. [17]. The mechanism developed was based on a previously published benzene model [18]. Ignition delay times (IDTs) were also measured in shock tube studies for various equivalence ratios at pressures varying from 1.95 to 8.85 atm [19]. An IDT, defined as the time interval between the initiation of a combustion process and the first energy release, is a measure of global reactivity, and such data provides a modeling target and is used for engine optimization [20]. These studies focused at temperatures above 1400 K. A more recent study expanded the available data to temperatures lower than 900 K, over a pressure range of 14–59 atm [21], while lower temperature measurements (600–900 K) were completed in a rapid compression machine (RCM) study [22]. Similarly, IDT data were measured at temperatures close to 1000 K for pressures in the range 25–45 atm, for fuel-lean and fuel-rich mixtures [23]. In addition to the models mentioned previously, which focused on ideal reactors, another detailed toluene mechanism of 141 species and 743 reactions was developed [24] utilizing additional experimental data measured in premixed and counter-flow flames. The two initial models reported above [15,16], have been, and still are, subjected to optimization by studies that followed [25–28].

IDTs of multi-component (two or more) fuels containing toluene have also been widely studied. The first of these investigated stoichiometric blends of 1:1 toluene/*n*-heptane and toluene/*iso*-octane mixtures in an RCM at 4 and 12 bar, reaching temperatures as low as 650 K [29]. Subsequently, the concentration of toluene was increased to 72% (vol.) with 28% *n*-heptane in a high-pressure shock tube (HPST) study [30] that focused on both fuel-lean and stoichiometric mixtures at various pressures, offering six sets of IDT data in the intermediate temperature region. This work was published with an accompanying study that utilized the experimental data for modeling purposes, developing a model for binary TRF mixtures [31]. Moreover, mixtures of toluene/*iso*-octane and toluene/*n*-heptane (10/90 and 40/60%vol.) were measured in a shock tube study at 40 bar at two equivalence ratios ($\varphi = 0.5$ and 1.0) [32]. Recently, toluene/dimethyl ether (DME) mixtures were investigated at several blending ratios ranging from 100% toluene to 100% DME, in both a HPST and in an RCM, using DME as a radical initiator [33].

Despite the systematic effort and the wide range of studies available, accurate predictions of toluene oxidation remain challenging. The issue is manifested in that most literature models are unable to reproduce experimental data at lower temperatures. In this context, the present study, like others before [27–31], focuses

on blending toluene with a very reactive and well characterized fuel, namely *n*-heptane, to increase mixture's reactivity and to extend the available experimental data to a wider range of conditions.

This study provides novel experimental ignition delay time data at conditions that have not previously been investigated, measuring both at low temperatures and high toluene concentrations in an attempt to bridge the observed gap in the literature. Measurements include three mixtures (50%, 75% and 90% vol. toluene concentration with the balance being *n*-heptane) at fuel-lean ($\varphi = 0.5$), stoichiometric ($\varphi = 1.0$) and fuel-rich ($\varphi = 2.0$) conditions at 10 and 30 bar over the temperature range of 650–1450 K. The detailed conditions of the mixtures investigated are provided in Table 1. The experiments were carried out in the high-pressure shock tube (HPST) and in a rapid compression machine (RCM) at the National University of Ireland, Galway (NUIG). The devices have been used in a complementary way to span the desired temperature range. Furthermore, to investigate the synergies of toluene and *n*-heptane in the reactivity of the TRF mixtures and to provide a detailed kinetic insight to the observed trends, the LLNL TRF detailed kinetic mechanism is utilized. The mechanism performance against the herein obtained data is assessed for both the original mechanism [33] as well as for the recently updated version [34,35], and the latter is found to yield improved and an overall good agreement. Sensitivity and reaction path analyses have been performed to delineate the key kinetic processes which control the oxidation of the mixtures considered under the reported conditions.

2. Experimental setup

2.1. High pressure shock tube

Ignition delay times at higher temperatures (800–1400 K) were measured in the HPST facilities of NUIG. The experimental setup has been described previously [36], thus it will be only briefly described here. The tube consists of two separate sections; the driven section, where the mixture sample is loaded, and the driver section where He or He/N$_2$ is introduced. These sections are 5.73 m and 3 m long respectively and are separated by a 3 cm long double-diaphragm (middle) section. The aluminum diaphragms are pre-scored to ensure uniform bursting. After the mixture is introduced into the driven section, the driver and middle sections are filled with He and/or N$_2$ to roughly half of the driver gas pressure. The driver section alone is then filled to the driver pressure. The gas from the middle section is evacuated and the pressure difference is sufficiently high to burst the diaphragms. The high-pressure driver gas expands rapidly into the driven section creating a shock wave that heats and compresses the mixture to the desirable conditions. Shock velocities are measured by interpolating the shock arrival time at PCB 113B24 pressure transducers along the driven section. A 603B Kistler pressure transducer is used to monitor the pressure of the gas at the endwall. The ignition delay time is defined as the time difference between the arrival of the shock wave at the endwall and the ignition event, measured by a sharp rise in pressure on ignition. The mixture was prepared by controlling the partial pressure of each constituent species in a stainless-steel mixing tank, while ensuring that it did not exceed a value of at least half of its vapor pressure. A heating system was installed on the mixing tank and the piping leading to the HPST to ensure that the fuel would remain in the vapor phase.

The entire experimental apparatus as well as the manifolds, piping and mixing vessel were heated to 60°C but not higher, to avoid overheating damage to the equipment (pressure transducers, gauges, etc.).

Table 1
Detailed conditions of the experimentally investigated mixtures.

Toluene Heptane ratio	Mole fraction (%)					
	C_7H_8	C_7H_{16}	O_2	N_2	Ar	Phi
50:50	1.03	1.03	20.57	77.37 (15.47)	(61.9)	1
50:50	0.52	0.52	20.8	78.17 (23.45)	(54.72)	0.5
50:50	2.01	2.01	20.16	75.82	–	2
75:25	1.62	0.54	20.55	77.30 (17.77)	(59.53)	1
75:25	0.82	0.27	20.77	78.14 (24.23)	(53.91)	0.5
75:25	3.18	1.06	20.11	75.66	–	2
90:10	2.01	0.22	20.53	77.24	–	1
90:10	1.02	0.11	20.76	78.11	–	0.5
90:10	3.93	0.44	20.08	75.55	–	2

*Numbers in parenthesis correspond to N_2 mole fraction when Argon is also used as diluent in the respective RCM cases for the intermediate temperature regime (830–1000 K).

2.2. Rapid compression machine

The RCM used in this study is one of the twin RCMs currently in operation at NUIG. It is the original RCM built at Shell [37] and later re-commissioned at NUIG [38]. Two opposite-facing pistons are pushed forward to volumetrically compress a fuel mixture. At the end of compression (∼16 ms), the pistons are locked and maintain a constant reactor volume. The RCM has a 168 mm stroke and a 38.2 mm bore. The position of the pistons is monitored with a Positek P100 linear inductive position sensor that is within the hollow connecting rod. The pressure inside the reaction chamber is measured using a Kistler 6045a mounted in the reaction chamber wall. A Kistler 5018 is used to amplify the pressure trace, while a Sigma 90 oscilloscope by Nicolet Technologies sampling at 20 kHz and 12-bit resolution is used for recording the traces. The pressure traces are filtered by a hardware Butterworth low-pass filter with a cut-off frequency of 3 kHz, after amplification. The compression ratio of the RCM, defined as the ratio of the density before and after compression is approximately 10. The ignition delay time is defined as the time of peak pressure at the end of compression and the maximum pressure rise due to chemical reactions. Different compressed-gas temperatures were achieved by varying the initial temperature in the chamber. An electrical heating system is used which has been optimized to minimize stratification in the chamber. More detailed description of the heating system installation was published previously [39]. The maximum initial temperature used was 105°C to avoid degradation of the seals inside the machine. Nitrogen was used as a sole diluent for the low-temperature measurements (650–830 K), while argon was added in the mixtures in the higher temperature regime (830–1000 K). Throughout the measurements the deviation from the desired compressed pressure was maintained below 1%. The pistons used in this study are creviced leading to a suppression of the roll-up vortices that otherwise form within the boundary layer gas, offering higher homogeneity in the mixture. They are a modified version of the pistons described previously [40]. *n*-Heptane was supplied by TCI UK with a purity of 99%. Toluene was supplied by Sigma Aldrich with a purity of 99.9%. None of the fuels were subjected to any further purification process. The blended samples were made by mass on a high precision scale. Nitrogen, argon and oxygen were provided by BOC Ireland. Each measurement in the RCM was repeated three times to ensure repeatability.

2.3. Experimental issues

In this study three blending ratios of high toluene content were measured. The high toluene concentration increases the deposits of soot and other residues in the experimental facility, e.g. in the RCM reaction chamber. Previous studies reported an early heat release and the occurrence of pre-ignition due to the presence of such deposits [21], while another study [33] overcame this problem by performing three consecutive oxygen shots after each experiment in the RCM. This proved to be a good method to clean the chamber and to ensure repeatability in IDT measurements. In the present work the fuel-rich mixtures (i.e. $\varphi = 2.0$) and high (i.e. 90%) toluene content mixtures were not studied, due to similar difficulties. In particular, it was found that the consecutive repeated shots for these cases resulted in higher IDT compared to the initial experiment. To solve this, the method reported in [33] was used but resulted in no observed ignition.

Regarding the HPST measurements the only issue observed (see point in circle in Fig. 1(c)). This has been reported in previous HPST studies and may be caused by inhomogeneous ignition [41–43] as ignition delay times reach values close to 10 ms.

3. Chemical kinetic modeling

In this work, the LLNL model was adopted as published in [36], while an updated version with modifications to the *n*-heptane portion from [37] and the toluene sub-mechanism from [35] was also utilized for comparison. The main modifications of the *n*-heptane mechanism include updated isomerization reactions for the heptyl radicals, as well as updates in the rates for cyclic ether formation. A detailed discussion of the modified parts is provided in [34,35]. The model includes 1426 species and 6128 reactions. Simulations were carried out utilizing the Aurora module of CHEMKIN-PRO [44] assuming constant volume conditions. Heat loss effects due to the facility for the RCM simulations, as described in [45], are included in the simulations. The input files for the RCM simulations are provided as Supplementary material.

4. Results and discussion

The measured ignition delay times for all conditions are plotted in Fig. 1 allowing for a comparison of many different variables. Each row contains measurements for a certain equivalence ratio with $\varphi = 0.5$ in the top row, $\varphi = 1.0$ in the middle and $\varphi = 2.0$ in the bottom row. Accordingly, the columns present measurements for mixtures with respect to their toluene content in ascending order, i.e. toluene:*n*-heptane ratio of 50:50 (left), 75:25 (middle) 90:10 (right).

Interestingly, a comparison along the y-axis (vertically) shows that the IDTs measured at 10 bar are almost insensitive to variations in equivalence ratio at temperatures above 1150 K. This behavior is less pronounced as the pressure increases and can be observed only at temperatures above 1250 K. Increasing the toluene concentration enhances this effect as data are sensitive to temperature for T > 1050 K for the low-pressure measurements. As temperatures decrease beyond these thresholds the fuel-lean cases have the longest IDTs. Another important observation can be made for
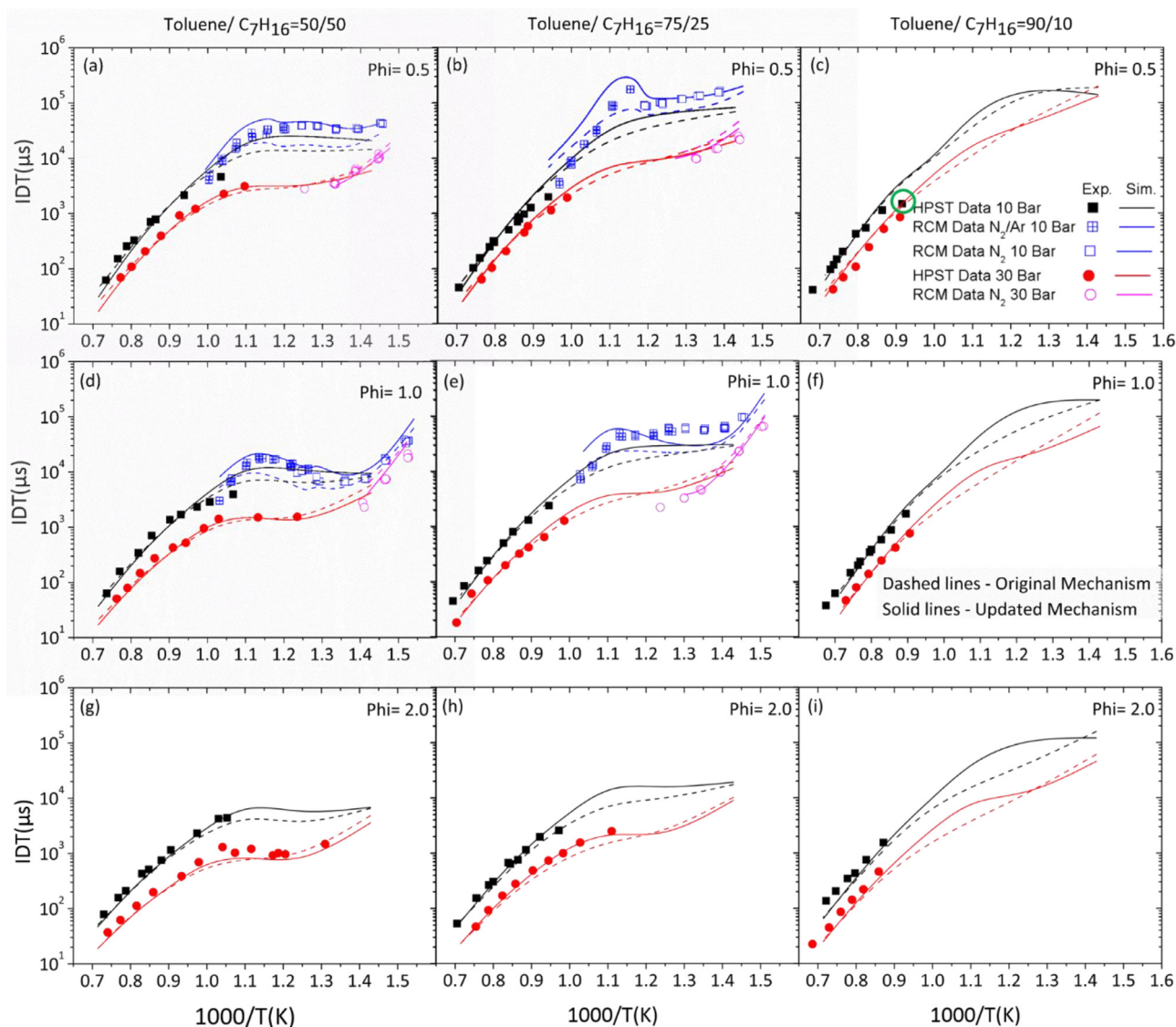
Fig. 1. Experimentally determined HPST (closed symbols) and RCM data (open symbols) versus simulations using the original LLNL TRF mechanism (dashed lines) and the updated mechanism (solid lines) Square symbols refer to experiments at 10 bar and circle symbols to those at 30 bar. Fig. 1 (c), (f), (g), (h), and (i) contain no RCM data. Point in green circle posed pre-ignition.

the 90:10 mixture ratio at 10 bar, where the IDT for the fuel-lean and the stoichiometric cases coincide, while the fuel-rich mixtures have significantly longer IDTs at low pressures. At 30 bar, the fuel-rich and stoichiometric mixtures coincide, while the fuel-lean mixture has notably shorter IDTs.

A comparison of the results in the x-direction (horizontally (a) → (c), (d) → (f) and (g) → (i)) show an increase in IDTs with increasing toluene content. However, this increase is more pronounced at lower temperatures and as the equivalence ratio (φ) increases. As discussed previously, fuel-rich mixtures ($\varphi = 2.0$) and mixtures with high toluene content (90:10) were not measured in an RCM, therefore Fig. 1(c), (f), (g), (h) and (i) contain no RCM data.

Regarding the performance of the mechanisms, Fig. 1(a) shows that the updated mechanism predicts longer IDTs in the low-pressure case yielding an improved performance against experimental data at lower temperatures. Both the HPST and the RCM data are well simulated. The modifications made to the mechanism do not affect its performance at 30 bar. Increasing the toluene concentration in the mixture to 75% naturally leads to longer predicted IDTs, as expected, Fig. 1(b). The updated version of the mecha-

nism predicts longer IDTs, compared to the original mechanism, at lower temperatures. In the NTC region the updates result in longer predicted IDTs. In general, the modifications have resulted in only a small change in the mechanism performance at high pressures with generally improved predictions observed.

Figure 1(d)–(f) show the stoichiometric measurements for all three mixture ratios. The updated model again predicts longer IDTs than the original mechanism, showing improved agreement compared to the reported data at temperatures below 1000 K. In the high temperature region, no difference in the performance of both models is observed. Both mechanisms, however, fail to capture the NTC behavior of the 75:25 mixture ratio Fig. 1(e), predicting shorter IDTs. As in the fuel-lean case, the 90:10 mixture shows only a small sensitivity to the mechanism modifications, Fig. 1(f).

As described earlier, the 90:10 mixtures were not measured in the RCM due to repeatability issues. The same problem occurred also in the fuel-rich cases, therefore only the HPST data are presented in Fig. 1(g)–(i). For the 50:50 and the 75:25 mixture the agreement is very good for all measurements. The updated mechanism captures well the IDTs at temperatures close to 900 K in the
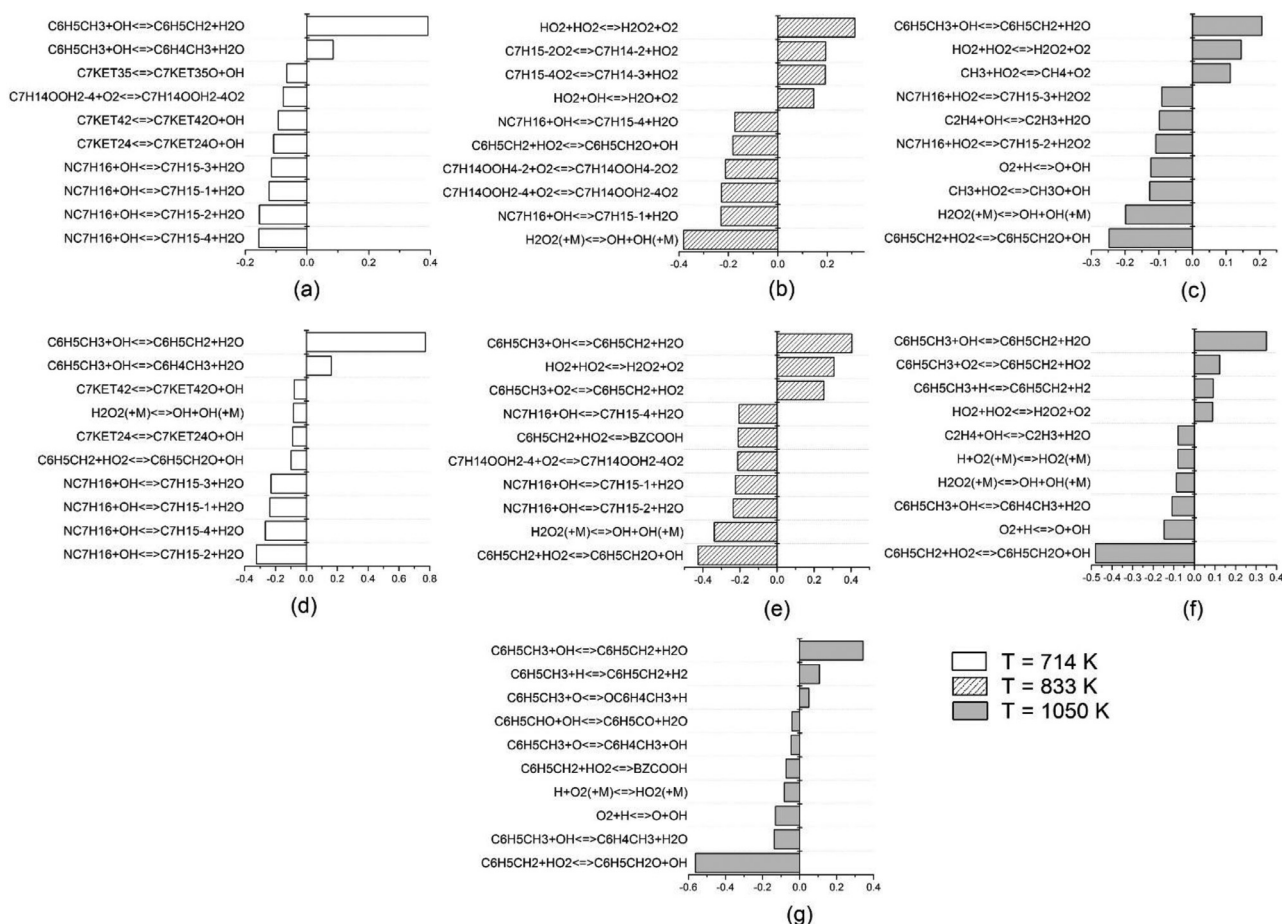
Fig. 2. Sensitivity analysis for ignition delay times at different toluene/n-heptane mixing ratios and temperatures for stoichiometric mixtures. (a)–(c): mixing ratio at 50:50; (d)–(f) mixing ratio at 75:25; (g) mixing ratio at 90:10.

30 bar case. Nonetheless, a small over-prediction for the 10 bar case is observed in the low temperature regime.

5. Sensitivity and reaction path analysis

A sensitivity analysis was performed for the ignition delay times at several conditions for the stoichiometric mixtures, with the results shown in Fig. 2, (a)–(c) for a toluene/heptane mixing ratio of 50:50, (d)–(f) for a mixing ratio of 75:25 and (g) for a mixing ratio of 90:10. The A factor of each reaction was increased and decreased by a factor of two (k_+ and k_-), leading to the perturbed ignition delay times (τ_+ and τ_-). The sensitivity coefficient (S) is calculated as:

$$S = \frac{\ln(\tau_+/\tau_-)}{\ln(k_+/k_-)} = \frac{\ln(\tau_+/\tau_-)}{\ln(2/0.5)}$$

Therefore, a positive sensitivity coefficient indicates an inhibiting effect upon the reactivity from a specific reaction, and vice versa for a negative coefficient. Over the temperature range of the experimental studies of this work, n-heptane is more reactive than toluene, especially at low and intermediate temperatures. n-Heptane has low temperature chain branching channels [34] that produce $\dot{O}H$ radicals. All of the heptyl-peroxy radicals can undergo intramolecular hydrogen transfer via low energy transition states, and the subsequent reaction sequences eventually lead to chain branching. This has also been indicated by the appearance of hydrogen abstraction and the low temperature reactions of n-heptane among the most promoting reactions in Fig. 2(a), (b), (d) and (e). At intermediate temperatures, chain propagat-

ing channels such as the concerted $H\dot{O}_2$ elimination reactions from $R\dot{O}_2$ radicals and cyclic ether + $\dot{O}H$ radical formation from hydroperoxy-alkyl ($\dot{Q}OOH$) radicals become more competitive than $\dot{Q}OOH$ radical addition to molecular oxygen resulting in negative temperature coefficient (NTC) behavior. These reactions become more sensitive when the relative concentration of n-heptane is higher in the fuel mixture, as shown in Fig. 2(b). At high temperatures, the hydrogen abstraction reactions by $H\dot{O}_2$ radicals are enhanced and produces H_2O_2 that decomposes into two $\dot{O}H$ radicals, which in turn is a chain-branching process. Abstraction reactions by $H\dot{O}_2$ radicals also show negative sensitivity coefficients, but again only at the highest concentration of n-heptane in the fuel mixture, Fig. 2(c).

In general, the toluene chemistry dominates the reactivity of the fuel mixtures over the entire temperature range shown in Fig. 2. This is because the reactivity of the fuel mixture not only depends on the reaction flux going through chain branching pathways that produce reactive radicals, but also depends on the branching ratio of the consumption pathways for those radicals. Under these conditions, toluene is a strong competitor for $\dot{O}H$ radicals despite it being much less reactive than n-heptane. Figure 2 shows that the hydrogen abstraction reactions from toluene inhibit reactivity at most conditions, except for the 50:50 mixture, where the n-heptane chemistry becomes more important.

The major reaction pathways in the oxidation of toluene are shown in Fig. 3, which is based on calculations for mixtures with a 50:50 ratio, at $\varphi = 1.0$, $p = 10$ bar and for $T = 690/870/1100/1400$ K. Toluene does not have low temperature chain branching channels. Hydrogen abstraction from toluene mainly occurs at the benzylic
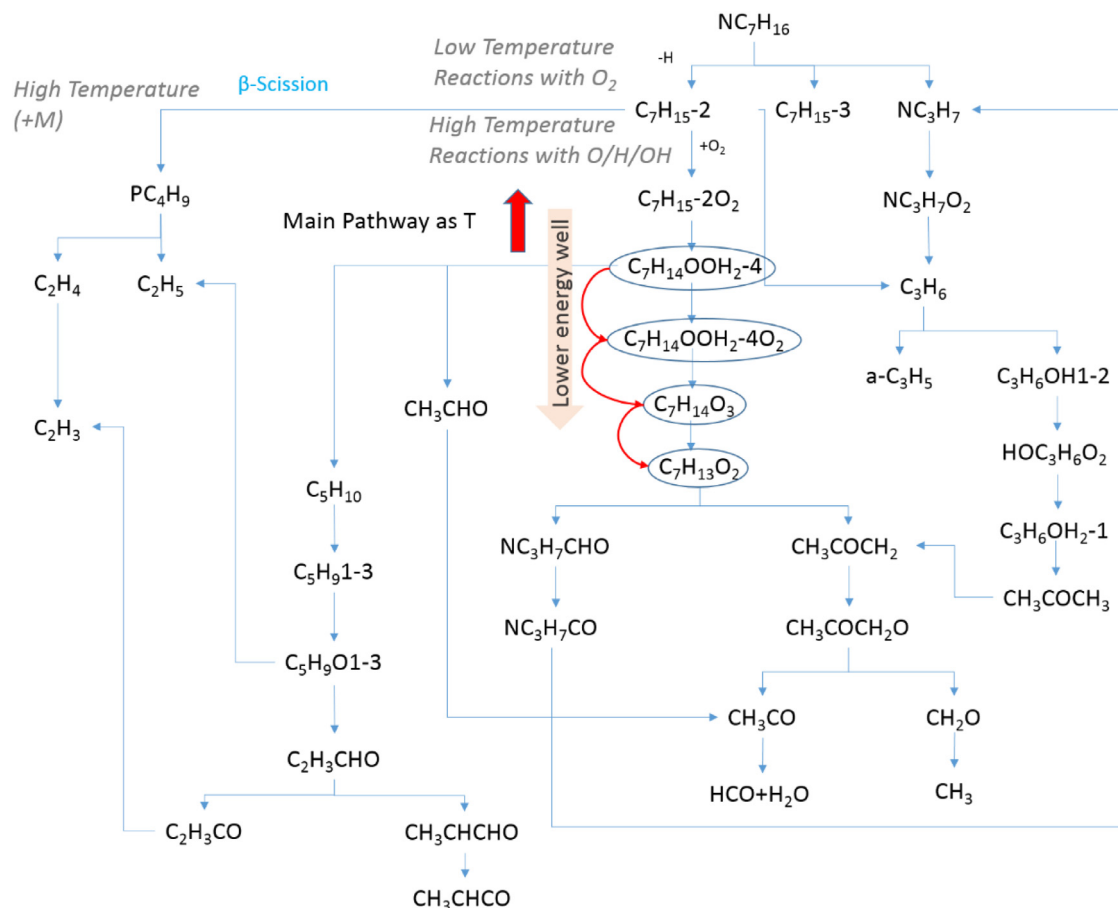
Fig. 3. Toluene oxidation route as obtained by reaction path analysis at 20% of fuel consumption for mixture ratio 50:50, φ = 1.0 at p = 10 bar and for T = 690/870/1100/1400 K.

site and produces benzyl radicals (see blue frame in Fig. 3). Benzyl is a relatively stable radical (ΔH_f (0 K) = 229.0 ± 4 kJ/mol [46]). The self-recombination of benzyl radicals is one of the major consumption pathways at low temperature, which is a chain terminating reaction and largely inhibits the overall reactivity (see yellow frame in Fig. 3). Another consumption channel of benzyl is through the reactions with $H\dot{O}_2$ radicals, either through recombination-decomposition or chemically activated paths, which produce benzoxyl radicals and $\dot{O}H$ radicals (see green frame in Fig. 3). The chemically activated paths are enhanced as the temperature rises and were found to be sensitive at the current conditions (see also Fig. 2(c), (e)–(g)). This also partly explains why toluene chemistry is less sensitive when the mixing ratio is 50:50. Benzyl radicals are mostly consumed by reacting with $H\dot{O}_2$ radicals that are largely produced from the concerted elimination of heptyl-peroxy radicals, producing more reactive $\dot{O}H$ radicals. Therefore, the production of benzyl radicals has a lesser inhibiting effect on the reactivity for the conditions presented in Fig. 2(b), (c) and its recombination is not shown among the most sensitive reactions. However, the chain terminating reaction of benzyl with $H\dot{O}_2$ radicals that produces toluene and oxygen is also enhanced at higher temperatures and thus inhibits reactivity. This reaction competes with the chain propagation process that produces $\dot{O}H$ radicals and thus has positive sensitivity coefficients. It should also be noted that this reaction becomes sensitive only when the production of benzyl and $H\dot{O}_2$ radicals are comparable within a certain degree, as show in Fig. 2(e) and (f).

Besides the toluene oxidation chemistry which is the primary topic in the present work, n-heptane oxidation is of large importance to the ignition delay time simulations, hence, a snapshot of the major chemical routes for the same conditions with that of toluene is given in Fig. 4.

6. Conclusions

The purpose of this work is twofold as it aims to (a) provide novel experimental ignition delay time data of toluene/n-heptane mixtures under conditions relevant to novel engine operation, which has not been reported before, and (b) to interpret the effect of the mixing ratio of toluene/n-heptane on the measured TRF IDT values, utilizing computational tools i.e. sensitivity and reaction flow analysis based on a detailed kinetic mechanism from the literature. In particular, the LLNL TRF model is used, both the original and the most recently updated version.

Experimental data have revealed that IDTs were in-sensitive to changes in equivalence ratio at higher temperatures. This behavior was less pronounced at higher pressures, starting at higher temperatures, but was enhanced with increasing toluene content. At low temperatures, the fuel-lean mixtures showed the longest IDTs. The opposite was observed for higher temperatures, where the fuel-lean mixtures were faster compared to stoichiometric and fuel-rich ones.

Computations demonstrated the improved agreement of the updated LLNL model compared to the current dataset; the updated model reproduces the experimentally observed longer IDTs in the low and intermediate temperature regime, presenting an overall improved performance, while it retains the original model's good performance in the high temperature regime. Reaction path and sensitivity analyses have shown that toluene inhibits reactivity, since it competes with n-heptane for $\dot{O}H$ radicals, resulting in the formation of relatively stable benzyl radicals rather than the production of heptyl radicals and heptyl-peroxyl radicals which would subsequently lead to chain-branching at low temperatures. This effect is less pronounced in the 50:50 mixture as the large quantity of $H\dot{O}_2$ radicals formed from heptyl-peroxy radical decomposition

Fig. 4. N−Heptane oxidation route as obtained by reaction path analysis at 20% of fuel consumption for mixture ratio 50:50, at $\varphi = 1.0$, $p = 10$ bar and for $T = 690/870/1100/1400$ K.

react with benzyl radicals resulting in the production of reactive $\dot{O}H$ radicals.

This paper provides novel experimental data that could serve in the validation of tuned toluene kinetic models in future endeavors. The validation with the currently existing models provides a good insight regarding the performance of the toluene models and the chemical interactions between toluene and *n*-heptane.

Supplementary materials

Supplementary material associated with this article can be found, in the online version, at doi:10.1016/j.combustflame.2018.10.024.

References

[1] W.J. Pitz, Charles J. Mueller, Recent progress in the development of diesel surrogate fuels, Prog. Energy Combust. Sci 37 (2011) 330–350.

[2] American Society of Testing Materials. d-2699 and d-2700. ASTM Research Method ASTM D 908 – 56 and ASTM Motor Method ASTM D 357 – 56, 1956.

[3] W.G. Lovell, Knocking characteristics of hydrocarbons, Ind. Eng. Chem. 40 (12) (1948) 2388–2438.

[4] N. Morgan, A. Smallbone, A. Bhave, M. Kraft, R. Cracknell, G. Kalghatgi, Mapping surrogate gasoline compositions into RON/MON space, Combust. Flame 157 (6) (2010) 1122–1131, doi:10.1016/j.combustflame.2010.02.003.

[5] C.K. Westbrook, M. Sjöberg, N.P. Cernansky, A new chemical kinetic method of determining RON and MON values for single component and multicomponent mixtures of engine fuels, Combust. Flame (2018), doi:10.1016/j.combustflame.2018.03.038.

[6] G.T. Kalghatgi, Developments in internal combustion engines and implications for combustion science and future transport fuels, Proc. Combust. Inst. 35 (1) (2015) 101–115, doi:10.1016/j.proci.2014.10.002.

[7] S.M. Sarathy, A. Farooq, G.T. Kalghatgi, Recent progress in gasoline surrogate fuels, Progr. Energy Combust. Sci. 65 (2018) 67–108, doi:10.1016/j.pecs.2017.09.004.

[8] J.A. Badra, N. Bokhumseen, N. Mulla, S.M. Sarathy, A. Farooq, G.T. Kalghatgi, P. Gaillard, A methodology to relate octane numbers of binary and ternary *n*-heptane, iso-octane and toluene mixtures with simulated ignition delay times, Fuel 160 (2015) 458–469, doi:10.1016/j.fuel.2015.08.007.

[9] T. Javed, C. Lee, M. AlAbbad, K. Djebbi, M. Beshir, J. Badra, H.J. Curran, A. Farooq, Ignition studies of *n*-heptane/iso-octane/toluene blends, Combust. Flame 171 (2016) 223–233, doi:10.1016/j.combustflame.2016.06.008.

[10] American Petroleum Institute. A.P.I. Research Project 45. History of the American Petroleum Institute, ASTM Special Technical Publication No. 225; 1941.

[11] V. Knop, M. Loos, C. Pera, N. Jeuland, A linear-by-mole blending rule for octane numbers of *n*-heptane/iso-octane/ toluene mixtures, Fuel 115 (2014) 666–673, doi:10.1016/j.fuel.2013.07.093.

[12] G.T. Kalghatgi, H. Babiker, J. Badra, A simple method to predict knock using toluene, N-Heptane and Iso-Octane Blends (TPRF) as gasoline surrogates, SAE Int. J. Engines 8 (2) (2015) 505–519.

[13] W.K. Metcalfe, S. Dooley, F.L. Dryer, Comprehensive detailed chemical kinetic modeling study of toluene oxidation, Energy & Fuels 25 (11) (2011) 4915–4936.

[14] K. Brezinsky, T.A. Litzinger, I. Glassman, The high temperature oxidation of the methyl side chain of toluene, Int. J. Chem. Kinet. 16 (1984) 1053–1074.

[15] P. Dagaut, G. Pengloan, A. Ristori, Oxidation, ignition and combustion of toluene: experimental and detailed chemical kinetic modeling, Phys. Chem. Chem. Phys. 4 (2002) 1846–1854.

[16] J.L. Emdee, K. Brezinsky, I. Glassman, A kinetic model for the oxidation of toluene near 1200 K, J. Phys. Chem. 96 (1992) 2151–2161.

[17] R. Bounaceur, I. Da Costa, R. Fournet, F. Billaud, F. Battin-Leclerc, Experimental and modeling study of the oxidation of toluene, Int. J. Chem. Kinet. 37 (1) (2004) 25–49, doi:10.1002/kin.

[18] I. Da Costa, R. Fournet, F. Billaud, Battin-Leclerc, Experimental and modeling study of the oxidation of benzene F, Int. J. Chem. Kinet. 35 (2003) 503–524.

[19] A. Burcat, C. Snyder, T. Brabbs, NASA Technical Memorandum 87312, Ignition Delay Times of Benzene Toluene with Oxygen in Argon Mixtures, National Aeronautics and Space Administration (NASA), Washington, D.C., 1986.

[20] S. Burden, A. Tekawade, M.A. Oehlschlaeger, Ignition delay times for jet and diesel fuels: constant volume spray and gas-phase shock tube measurements, Fuel 219 (2018) 312–319, doi:10.1016/j.fuel.2018.01.113.

[21] D.F. Davidson, B.M. Gauthier, R.K. Hanson, Shock tube ignition measurements of iso-octane/air and toluene/air at high pressures, Proc. Combust. Inst. 30 (2005) 1175–1182.

[22] A. Roubaud, R. Minetti, L.R. Sochet, Oxidation and combustion of low alkyl-benzenes at high pressure: comparative reactivity and auto-ignition Combust, Flame 123 (2000) 535–541.

[23] G. Mittal, C.J. Sung, Autoignition of toluene and benzene at elevated pressures in a rapid compression machine, Combust. Flame 150 (2007) 355–368.

[24] R.P. Lindstedt, L.Q. Maurice, Detailed kinetic modelling of toluene combustion, Combust. Sci. Technol. 120 (1–6) (1996) 119–167, doi:10.1080/00102209608935571.

[25] R. Sivaramakrishnan, R.S. Tranter, K. Brezinsky, High-pressure, high-temperature oxidation of toluene, Combust. Flame 139 (2004) 340–350.

[26] S.D. Klotz, K. Brezinsky, I. Glassman, Modeling the combustion of toluene – butane blends, Proc. Combust. Inst. 27 (1998) 337–344.

[27] W.H. Yuan, Y.Y. Li, P. Dagaut, J.Z. Yang, F. Qi, Investigation on the pyrolysis and oxidation of toluene over a wide range conditions. II. A comprehensive kinetic modeling study, Combust. Flame 162 (2015) 3–21.

[28] W.H. Yuan, Y.Y. Li, P. Dagaut, J.Z. Yang, F. Qi, Investigation on the pyrolysis and oxidation of toluene over a wide range conditions. I. Flow reactor pyrolysis and jet stirred reactor oxidation, Combust. Flame 162 (2015) 22–40.

[29] G. Vanhove, G. Petit, R. Minetti, Experimental study of the kinetic interactions in the low-temperature autoignition of hydrocarbon binary mixtures and a surrogate fuel, Combust. Flame 145 (2006) 521–532.

[30] J. Herzler, M. Fikri, K. Hitzbleck, R. Starke, C. Schulz, P. Roth, G.T. Kalghatgi, Shock-tube study of the autoignition of *n*-heptane/toluene/air mixtures at intermediate temperatures and high pressures, Combust. Flame 149 (2007) 25–31.

[31] J.C.G. Andrae, P. Björnbom, R.F. Cracknell, G.T. Kalghatgi, Autoignition of toluene reference fuels at high pressures modeled with detailed chemical kinetics, Combust. Flame 149 (2007) 2–24.

[32] M. Hartmann, I. Gushterova, M. Fikri, C. Schulz, R. Schießl, U. Maas, Auto-ignition of toluene-doped *n*-heptane and iso-octane/air mixtures: High-pressure shock-tube experiments and kinetics modeling, Combust. Flame 158 (2011) 172–178.

[33] Y. Zhang, K.P. Somers, M. Mehl, W.J. Pitz, R.F. Cracknell, H.J. Curran, Probing the antagonistic effect of toluene as a component in surrogate fuel models at low temperatures and high pressures. A case study of toluene/dimethyl ether mixtures, Proc. Combust. Inst. 36 (2017) 413–421.

[34] M. Mehl, S. Wagnon, K. Tsang, G. Kukkadapu, W.J. Pitz, C.K. Westbrook, Y. Tsang, H.J. Curran, N. Atef, M.A. Rachidi, M.S. Sarathy, A. Ahmed, A comprehensive detailed kinetic mechanism for the simulation of transportation fuels 10th US National Combustion Meeting (2017), College Park, MD, United States

[35] G. Kukkadapu, D. Kang, S.W. Wagnon, K. Zhang, M. Mehl, M. Monge-Palacios, H. Wang, S. Goldsborough, C.K. Westbrook, W.J. Pitz, Kinetic modeling study of surrogate components for gasoline, jet and diesel fuels: C7-C11 methylated aromatics, Proceedings of the Combustion Institute (2018), doi:10.1016/j.proci.2018.08.016.

[36] H. Nakamura, D. Darcy, M. Mehl, C.J. Tobin, W.K. Metcalfe, W.J. Pitz, C.K. Westbrook, H.J. Curran, An experimental and modeling study of shock tube and rapid compression machine ignition of n-butylbenzene/air mixtures, Combust. Flame 161 (1) (2014) 49–64, doi:10.1016/j.combustflame.2013.08.002.

[37] W.S. Affleck, A. Thomas, An opposed piston rapid compression machine for preflame reaction studies, Proc. Inst. Mech. Eng. 183 (1969) 365–385.

[38] L. Brett, J. Macnamara, P. Musch, J.M. Simmie, Simulation of methane autoignition in a rapid compression machine with creviced pistons, Combust. Flame 124 (2001) 326–329.

[39] D. Darcy, H. Nakamura, C.J. Tobin, M. Mehl, W.K. Metcalfe, W.J. Pitz, C.K. Westbrook, H.J. Curran, A high-pressure rapid compression machine study of n-propylbenzene ignition, Combust. Flame 161 (2014) 65–74.

[40] J. Würmel, J.M. Simmie, CFD studies of a twin-piston rapid compression machine, Combust. Flame 141 (2005) 417–430.

[41] A.B. Mansfield, M.S. Wooldridge, H. Di, X. He, Low-temperature ignition behavior of iso-octane, Fuel 139 (2015) 79–86.

[42] Y. Uygun, S. Ishihara, H. Olivier, A high pressure ignition delay time study of 2-methylfuran and tetrahydrofuran in shock tubes, Combust. Flame 161 (10) (2014) 2519–2530.

[43] N. Atef, G. Kukkadapu, S.Y. Mohamed, M.Al. Rashidi, C. Banyon, M. Mehl, K.A. Heufer, E.F. Nasir, A. Alfazazi, A.K. Das, C.K. Westbrook, W.J. Pitz, L. Tianfeng, A. Farooq, S. Chih-Jen, H.J. Curran, S.M. Sarathy, A comprehensive iso-octane combustion model with improved thermochemistry and chemical kinetics, Combust. Flame 178 (2017) 111–134.

[44] http://www.reactiondesign.com/products/chemkin/chemkin-pro/.

[45] C.-J. Sung, H.J. Curran, Using rapid compression machines for chemical kinetics studies, Prog. Energy Combust. Sci. 44 (2014) 1–18.

[46] H. Hippler, J. Troe, Thermodynamic properties of benzyl radicals: enthalpy of formation from toluene, benzyl iodide, and dibenzyl dissociation equilibria, J. Phys. Chem. 94 (9) (1990) 3803–3806.